

Received:  
23 March 2020Revised:  
10 June 2020Accepted:  
15 July 2020<https://doi.org/10.1259/bjr.20200267>

Cite this article as:

Fiocchi F, Monelli F, Besutti G, Casari F, Petrella E, Pecchi A, et al. MRI of placenta accreta: diagnostic accuracy and impact of interventional radiology on foetal-maternal delivery outcomes in high-risk women. *Br J Radiol* 2020; **93**: 20200267.

## FULL PAPER

# MRI of placenta accreta: diagnostic accuracy and impact of interventional radiology on foetal-maternal delivery outcomes in high-risk women

<sup>1</sup>FEDERICA FIOCCHI, MD, <sup>1</sup>FILIPPO MONELLI, MD, <sup>2</sup>GIULIA BESUTTI, MD, <sup>1</sup>FEDERICO CASARI, MD, <sup>3</sup>ELISABETTA PETRELLA, MD, <sup>1</sup>ANNARITA PECCHI, MD, <sup>1</sup>CRISTIAN CAPORALI, MD, <sup>3</sup>EMMA BERTUCCI, MD, <sup>4</sup>STEFANO BUSANI, MD, <sup>5</sup>LAURA BOTTICELLI, MD, <sup>3</sup>FABIO FACCHINETTI, MD and <sup>1</sup>PIETRO TORRICELLI, MD

<sup>1</sup>Department of Radiology, Azienda ospedaliero- universitaria Policlinico di Modena, Modena, Italy

<sup>2</sup>University of Modena and Reggio Emilia, Clinical and Experimental Medicine PhD program, Modena, Italy

<sup>3</sup>Department of Medical and Surgical Sciences for Mothers, Children and Adults, Azienda ospedaliero - universitaria Policlinico di Modena, Modena, Italy

<sup>4</sup>Department of intensive care medicine, Azienda ospedaliero - universitaria Policlinico di Modena, Modena, Italy

<sup>5</sup>Department of Pathology, Azienda ospedaliero - universitaria Policlinico di Modena, Modena, Italy

Address correspondence to: Dr Filippo Monelli  
E-mail: [mofilippo@hotmail.it](mailto:mofilippo@hotmail.it)

Federica Fiocchi and Filippo Monelli have contributed equally to this study and should be considered as co-first authors.

**Objective:** To assess accuracy and reproducibility of MRI diagnosis of invasive placentation (IP) in high-risk patients and to evaluate reliability of MRI features. Secondary aim was to evaluate impact of interventional radiology (IR) on delivery outcomes in patients with IP at MRI.

**Methods:** 26 patients (mean age 36.24 y/o, SD 6.16) with clinical risk-factors and echographic suspicion of IP underwent 1.5 T-MRI. Two readers reviewed images. Gold-standard was histology in hysterectomised patients and obstetric evaluation at delivery for patients with preserved uterus. Accuracy and reproducibility of MRI findings were calculated.

**Results:** Incidence of IP was 50% (13/26) and of PP was 11.54% (3/26). MRI showed 100% sensitivity (95% CI = 75.3-100%) and 92.3% specificity (95% CI = 64.0-100%) in the diagnosis of IP. Gold-standard was histology in 10 cases and obstetric evaluation in 16. MRI findings with higher sensitivity were placental heterogeneity, uterine bulging and black intraplacental bands. Uterine scarring,

placental heterogeneity, myometrial interruption and tenting of the bladder showed better specificity. MRI inter-rater agreement with Cohen's K was 1. 11 patients among 14 with MRI diagnosis of IP received IR assistance with positive impact on delivery outcomes in terms of blood loss, red cells count, intensive care unit length of stay, days of hospitalisation and risk of being transfused.

**Conclusion:** MRI is an accurate and reproducible technique in prenatal diagnosis of IP. MRI helps planning a safe and appropriate delivery eventually assisted by IR, which positively affects foetal and maternal outcomes.

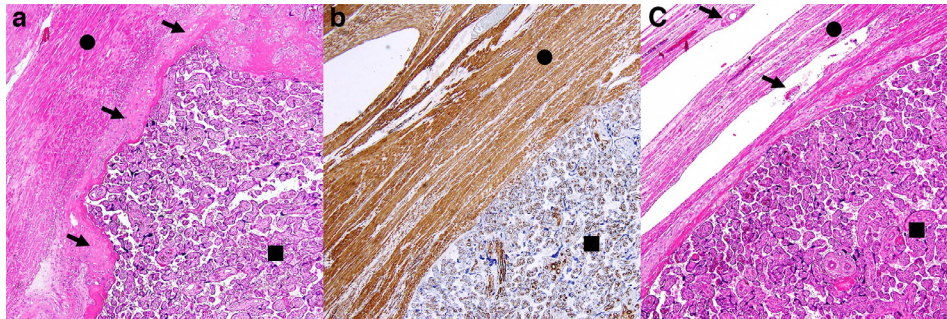
**Advances in knowledge:** The adoption of MRI evaluation in patients with high risk of invasive placentation allows a more accurate diagnosis in terms of both presence of the disease and its extension to or through or even beyond the myometrium. This led to a better dedicated delivery management with eventual adoption of interventional radiology with a global positive effect on foetal and maternal outcomes.

## INTRODUCTION

Placental adherence disorders are a relevant cause of maternal morbidity and mortality in peripartum period; among these, invasive placentation (IP) has the most severe clinical impact, which is related to width and depth of myometrial invasion.<sup>1,2</sup> IP affects about 0.1% of all pregnancies and it comprehends a spectrum of conditions characterised by direct attachment of chorionic villi to

the myometrium due to a defect of the spongiosus layer of decidua basalis, which causes increased placental-myometrial adhesion.<sup>3,4</sup> Three different entities, placenta accreta vera (PA), increta (PI) and percreta (PP) are described [Figure 1](#). IP is usually silent throughout pregnancy, but causes 1% of pregnancy related haemorrhages, about 1% of pregnancy related death and 29% of haemorrhages requiring hysterectomy.<sup>5-7</sup>

Figure 1. Three histological samples of human placenta. (A) Haematoxylin and eosin stain of placenta accreta vera: chorionic villi (black square) are attached to myometrium composed of spindle cells (black circle), throughout decidua basalis (black arrows) which is thinned, but not interrupted. (B) Desmin stain of a placenta increta: chorionic villi (black square) infiltrate the myometrium (black circle); decidua basalis cannot be identified. (C) Haematoxylin and eosin stain of placenta percreta: chorionic villi (black square and black arrows) penetrate through the myometrium (black circle) up to the uterine serosa.



Incidence of IP is growing in last decades due to an increasing incidence of risk factors,<sup>8–10</sup> namely placenta previa and surgical procedures on the myometrium such as caesarean sections (CS) or other uterine surgery including surgical pregnancy interruptions.<sup>11</sup> Prenatal diagnosis is crucial since in case of IP it is mandatory to plan a CS in a tertiary referral hospital for obstetric surgery with availability of blood products, neonatal–maternal intensive care unit and a skilled multidisciplinary team. In recent years, interventional radiology (IR) assistance through hypogastric or uterine artery occlusion and/or embolisation during delivery has been introduced<sup>12–15</sup> proving to be a safe procedure with few complications and a very low radiation dose administered to the foetus.<sup>16,17</sup>

The main tool for diagnosing IP is targeted ultrasonography performed between the 24th and 26th week,<sup>18</sup> whose specificity and sensitivity are both reported over 90%.<sup>19</sup> Nevertheless, diagnostic accuracy of targeted ultrasonography may be affected by operator experience, availability of patient detailed clinical history, posterior implantation of the placenta and obesity.<sup>20</sup> In last two decades, MRI emerged as a diagnostic tool to diagnose IP because, despite its overall equal or even slight lower accuracy,<sup>21</sup> it allows a precise description of width and depth of placental invasion. Moreover, MRI does not have the same limitation, and, in case of posterior placentation, obese patients and inconclusive ultrasound evaluation its use is suggested by international guidelines.<sup>22</sup> The appropriate time point to perform MRI is as close as possible to the 36th week as, an earlier MRI evaluation underestimates IP<sup>23</sup> and overestimates the presence of placenta previa due to normal ascension of the placenta into the uterus during pregnancy. A later MRI evaluation may overestimate IP and hamper the planning of IR-assisted delivery in females affected by IP.

The first aim of the present study was to assess accuracy and reproducibility of MRI diagnosis of IP in high-risk patients and to evaluate the most accurate feature of IP. In second instance the impact of interventional radiology assistance on delivery outcomes in patients diagnosed with IP at MRI was analysed.

## METHODS AND MATERIALS

### Study design

A retrospective observational study was conducted on a cohort of consecutive females at intermediate or high risk for IP who underwent to ultrasound evaluation, performed by a dedicated Obstetric Gynaecologist. The study was approved by the ethics committee of the university hospital of Modena and Reggio Emilia.

### Patients

From June 2013 to November 2018, 83 females with suspicion of IP were referred to the Gynaecology Department. The following risk factors were considered: placenta previa, multiple previous caesarean sections or other surgical uterine procedures, posterior placenta, high parity defined as more than four pregnancies, maternal age over 35 years and obesity defined as a BMI over 30. The patients received specific clinical examination and targeted ultrasonography evaluation performed by a dedicated Obstetric Gynaecologist. 26 out of 83 patients were included in the study due to high risk of IP and underwent MRI, which was scheduled before 38th gestational week.

### MRI examinations

All pelvic MRI examinations for placental evaluation were performed on a 1.5 T scanner (Philips Achieva, The Best, Netherlands) with 5-element cardiac synergy coil, after injection of an antiperistaltic drug and medium bladder filling. Imaging protocol included single-shot turbo spin echo  $T_2$  weighted (TSE) and steady-state free precession sequences (balanced turbo field-echo BTFE) performed on utero-placental sagittal, axial and coronal planes,  $T_1$  weighted high resolution isotropic volume examination fat-saturated (THRIVE) performed on uteroplacental axial and sagittal planes. Moreover, a diffusion-weighted echoplanar imaging (EPI) was performed in axial plane. Sequences parameters are reported in Table 1. In Figure 2a, normal placenta is depicted, and features of normal placentation are described.

### Images analyses

Two radiologists, dedicated to pelvic and gynaecological MRI, prospectively evaluated the exams. Readers assigned patients to

Table 1. Exam protocol

| Sequence (name)  | Sequence detail  | Acquired planes              |
|--|--|------------------------------|
| Single-shot TSE $T_2$ weighted   | RT/ET: 3293/80 ms<br>Slice thickness: 5 mm<br>Acquisition matrix: 264 × 220                        | Sagittal<br>Axial<br>Coronal |
| Three-dimensional high-resolution isotropic volume $T_1$ weighted fat-saturated (THRIVE) | RT/ET: 3.6/1.69 ms.<br>Slice thickness: 6 mm<br>Acquisition matrix: 124 × 110                      | Axial<br>Sagittal            |
| Steady-state free precession sequences (BTFE)  | RT/ET: 3.5/1.77 ms<br>Slice thickness: 5 mm<br>Acquisition matrix: 272 × 212                       | Sagittal<br>Axial<br>Coronal |
| DWI; EPI imaging single shot   | RT/ET: 3.584/71 ms<br>Slice thickness: 5 mm<br>Acquisition matrix: 104 × 85<br>B values: 0-400-800 | Axial                        |

BTFE, balanced turbo field-echo; DWI, diffusion-weighted imaging; EPI, echoplanar imaging; TSE, turbo spin echo. Exam protocol used. It was adapted to every woman, and in some cases, not every sequence could be performed.

three groups considering multiple radiological features of IP: non-IP, PA / PI and PP.

Specific features of IP (Figure 3) evaluated to formulate MRI diagnosis were: uterine bulging, placental signal heterogeneity, dark intraplacental bands, hyperintense placental lacunae, interruption of the myometrium and of inner myometrial layer, placental implant on previous CS uterine scar and tenting of the bladder.<sup>21,24-27</sup> Myometrium Interruption and tenting of the bladder should be considered a sign of extra uterine extension of placental elements typical of PP. PA and PI were considered the same pathology both at ultrasound and at MRI, since the difference between them is not possible at imaging.

### Interventional radiology

All patients with diagnosis of IP at MRI were planned for IR-assisted delivery with the aim to reduce blood loss and related foetal maternal complication. In angiography room, Fogarty occlusion catheters were placed in both hypogastric arteries at their most proximal division with an arterial access gained with Seldinger technique, paying attention to foetal dose exposure. Then, patients were transferred to the operating room, where the CS was performed after the arterial block; in case of difficult after birth, uterotonic drugs were administered. Foetal dose exposure was collected. Delivery-related foetal and maternal outcomes were registered: blood loss, haemoglobin lost in operating room, red cells transfusion, days spent in intense care unit, days of hospitalisation, need of transfusion and hysterectomy.

Figure 2. Patient n° 7, 39 y/o at 32nd week, at first pregnancy. Placenta previa with no IP. (A) Sagittal BTFE image of a previa posterior placenta. Internal cervical os (white arrow) and cervical canal (white circle). No uterine bulge and normal placental septae (empty arrow), which are thin hypointense lines located between placental lobes. (B) Axial T2 weighted TSE image. Placenta has an homogeneous intermediate T2 signal (white arrows) and lays on the myometrium (white arrowhead), normally thinned at advanced maternal age. BTFE, balanced turbo field-echo.

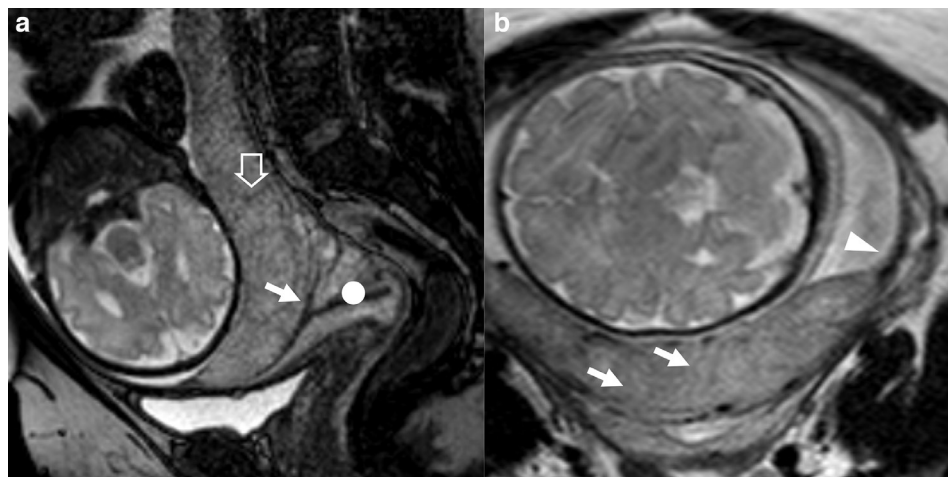
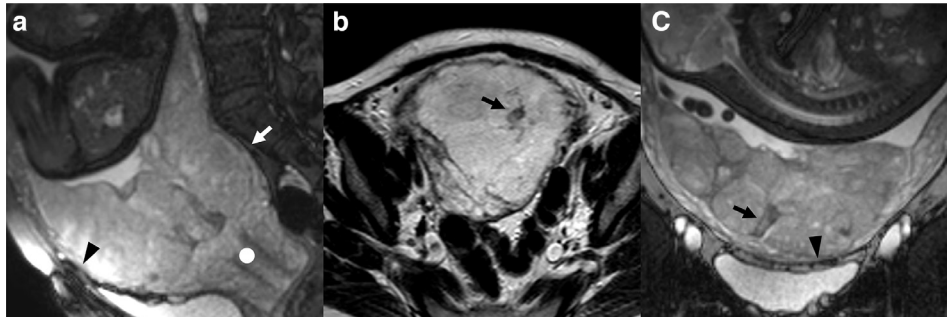


Figure 3. Patient n° 2, 40 y/o at 33rd week, at 11th pregnancy, with one previous CS. Placenta previa increta histologically confirmed. (A) sagittal BTFE, (B) axial T2 TSE, (C) BTFE coronal images. (A) uterine posterior bulging (white arrow) and implant of the placenta on uterine scar from previous caesarean section, where the myometrium is thinned (black arrowhead). No clear separation between placenta and the cervix (white circle). (B) nodular T2 black band (black arrow) in a mild heterogeneous portion of the placenta; (C) nodular and thick linear areas of hypointensity (black arrow) inside a very heterogeneous portion of the placenta and thinning of the inner myometrial layer (black arrowhead). BTFE, balanced turbo field-echo; TSE, turbo spin echo.



### Gold-standard

A twofold GS<sup>28</sup> was adopted because a precise differentiation between PA and PI is possible only in case of hysterectomy and consequent histopathological evaluation of both placenta and myometrium.<sup>29</sup> Placental histological examination has low reliability for IP assessment<sup>30</sup> and in case of uterus preservation, clinical evaluation of the obstetric surgeon during CS was adopted. In case of hysterectomy, the pathologist was blinded to MRI findings and radiological diagnosis, while in case of surgical GS, the obstetric surgeon was aware of it.

### Statistical analysis

Descriptive statistics were performed for all demographical variables. Numerical data were expressed as mean and standard deviation. Diagnostic performance is evaluated on the ROC curve and the area under the curve (AUC), specificity (SPEC), sensitivity (SEN), PPV and NPV with respective 95% confidence intervals (CI 0.95) were calculated for MRI diagnosis of IP, MRI diagnosis of PP and every specific feature of IP. Cohen's  $\kappa$  ( $\kappa$ ) statistic was calculated in the evaluation of interobserver agreement. According to the delivery management, females with MRI diagnosis of IP were subdivided into IR-assisted (IR-A) and IR-not assisted (IR-NA) groups.

### RESULTS

26 patients with intermediate-high risk of IP at targeted ultrasound underwent MRI: no females were excluded from the study. Five females required an emergency delivery before the planned CS because of foetal complications and three of them diagnosed with IP, could not be assisted with IR. Among 26 patients, 11 underwent hysterectomy and histological examination was performed on removed uterus. In 15 patients, whose uterus was preserved, surgical GS was adopted. At GS, IP was found in 13 patients with an incidence of 50%, and among these, 10 had PA/PI (38.46%) and 3 had PP (11.54%).

Clinicodemographical characteristics grouped for different diagnosis are reported in [Table 2](#).

[Table 3](#) summarises diagnostic accuracy and inter-rater agreement of MRI and MRI specific features evaluated. IP was diagnosed with MRI in 14 patients with 100% sensitivity (CI 0.95: 75.3–100%) and 92.3% specificity (CI 0.95: 64.0–100%), with one false positive case and no missed diagnosis. The most accurate MRI feature of IP in our case series has been placental heterogeneity followed by uterine bulging and interruption of the myometrium. PP was diagnosed in three patients

Table 2. Study population

|                         | All patients (26)    | Non-IP (13)         | IP (13)             | PA/PI (10)          | PP (3)               |
|-------------------------|----------------------|---------------------|---------------------|---------------------|----------------------|
| Age (years)             | 36.24 ( $\pm$ 6.16)  | 37.15 ( $\pm$ 5.26) | 35.33 ( $\pm$ 7.05) | 37.45 ( $\pm$ 6.47) | 28.29 ( $\pm$ 3.54)  |
| Gestational age (weeks) | 33.81 ( $\pm$ 5.36)  | 35.00 ( $\pm$ 2.35) | 32.62 ( $\pm$ 7.16) | 32.10 ( $\pm$ 7.84) | 34.33 ( $\pm$ 5.03)  |
| Previous pregnancies    | 3.35 ( $\pm$ 2.53)   | 2.46 ( $\pm$ 1.20)  | 4.23 ( $\pm$ 3.19)  | 4.80 ( $\pm$ 3.43)  | 2.33 ( $\pm$ 1.15)   |
| Parity                  | 1.54 ( $\pm$ 1.75)   | 0.92 ( $\pm$ 1.12)  | 2.15 ( $\pm$ 2.08)  | 2.40 ( $\pm$ 2.27)  | 1.33 ( $\pm$ 1.15)   |
| Uterine surgery °       | 1.23 ( $\pm$ 1.11)   | 1.00 ( $\pm$ 1.08)  | 1.46 ( $\pm$ 1.13)  | 1.60 ( $\pm$ 1.17)  | 1.00 ( $\pm$ 1.00)   |
| BMI *                   | 23.90 ( $\pm$ 17.52) | 23.82 ( $\pm$ 5.94) | 23.98 ( $\pm$ 5.91) | 24.22 ( $\pm$ 6.26) | 23.18 ( $\pm$ 22.95) |

BMI, body mass index; IP, invasive placentation; PA, placenta accreta vera; PP, placenta percreta.

Clinical characteristics of enrolled patients grouped for GS diagnosis. °Uterine surgery is the sum of every surgical event on the uterus including caesarean sections and surgical pregnancy interruptions; \* BMI is referred to the beginning of the pregnancy.

Table 3. Accuracy and interrater agreement of MRI

|  | SEN (%)           | SPEC (%)           | AUROC                | PPV (%)           | NPV (%)           | Cohen's K coefficient |
|--|-------------------|--------------------|----------------------|-------------------|-------------------|-----------------------|
| MRI                                    | 100<br>75,3–100   | 92,31<br>64,0–99,8 | 0,962<br>0,804–0,999 | 92,9<br>66,1–99,8 | 100<br>73,5–100   | 1,000<br>1,000–1,000  |
| MRI of placenta percreta               | 66,7<br>9,4–99,2  | 95,7<br>78,1–99,9  | 0,812<br>0,611–0,937 | 66,7<br>9,4–99,2  | 95,7<br>78,1–99,9 | 0,708<br>0,336–1,000  |
| Uterine Bulging                        | 92,3<br>64,0–99,8 | 84,6<br>54,6–98,1  | 0,885<br>0,698–0,976 | 85,7<br>67,2–98,2 | 91,7<br>61,5–99,8 | 0,766<br>0,519–1,000  |
| Placental Heterogeneity                | 100<br>75,3–100   | 100<br>75,3–100    | 1,000<br>0,868–1,000 | 100<br>75,3–100   | 100<br>75,3–100   | 0,769<br>0,524–1,000  |
| Dark intraplacental bands              | 84,6<br>54,6–98,1 | 76,9<br>46,2–95,0  | 0,808<br>0,606–0,934 | 78,6<br>49,2–95,3 | 83,3<br>51,6–97,9 | 1,000<br>1,000–1,000  |
| Hyperintense placental lacunae         | 61,5<br>31,6–86,1 | 58,3<br>27,7–84,8  | 0,599<br>0,386–0,788 | 61,5<br>31,6–86,1 | 58,3<br>27,7–84,8 | 0,516<br>0,183–0,849  |
| Interruption of the myometrium         | 84,6<br>54,6–98,1 | 100<br>75,3–100    | 0,923<br>0,749–0,991 | 100<br>71,5–100   | 86,7<br>59,5–98,3 | 0,846<br>0,643–1,000  |
| Interruption of inner myometrial layer | 100<br>75,3–100   | 61,5<br>31,6–86,1  | 0,808<br>0,606–0,934 | 72,2<br>46,5–90,3 | 100<br>63,1–100   | 0,462<br>0,100–0,824  |
| Implant on uterine scar                | 53,9<br>25,1–80,8 | 100<br>75,3–100    | 0,769<br>0,564–0,910 | 100<br>59,0–100   | 68,4<br>43,4–87,4 | 0,698<br>0,391–1,000  |
| Bladder tenting                        | 38,5<br>13,9–68,4 | 92,31<br>64,0–99,8 | 0,654<br>0,443–0,828 | 83,3<br>35,9–99,6 | 60,0<br>36,1–80,9 | 0,539<br>0,195–0,883  |

AUROC, area under the ROC curve; NPV, negative predictive value; PPV, positive predictive value; SEN, sensitivity; SPEC, specificity.

Cohen's K coefficient: < 0 less than chance agreement; 0.01–0.20 slight agreement; 0.21–0.40 fair agreement; 0.41–0.60 moderate agreement; 0.61–0.80 substantial agreement; 0.81–0.99 almost perfect agreement; 1 perfect agreement.

(Figure 4) with 66.7% sensitivity (CI 0.95: 9.4–99.2%) and 95.6% specificity (CI 0.95: 78.1–99.9%) with one false positive case. Moreover, MRI missed a PP, which was evaluated as PI but subsequently showed a focal placental percreta at GS (Figure 5).

MRI inter-rater agreement with Cohen's K was 1 (CI 0.95: 1.000–1.000).

Among patients with MRI diagnosis of IP, 3 were not assisted with IR and 11 patients were assisted with IR. In Table 4, there is a summary of their outcomes. IR-NA group lost 1269.70 ml more blood in the operating room (CI 0.95: 225.87–2313.53

Figure 4. patient n° 18, 32 y/o at 35th week, at third pregnancy, with two previous CS. Placenta previa percreta histologically confirmed. (A) BTFE axial and B) T1 GE coronal images. (A) penetration of the placental tissue through the myometrium which results interrupted (white arrowhead) and intraplacental nodular black band (white empty arrow) which correspond in B) to an hyperintense T1 spot (white arrow) representing a focus of haemorrhage typical of abnormal placentation. BTFE, balanced turbo field-echo.

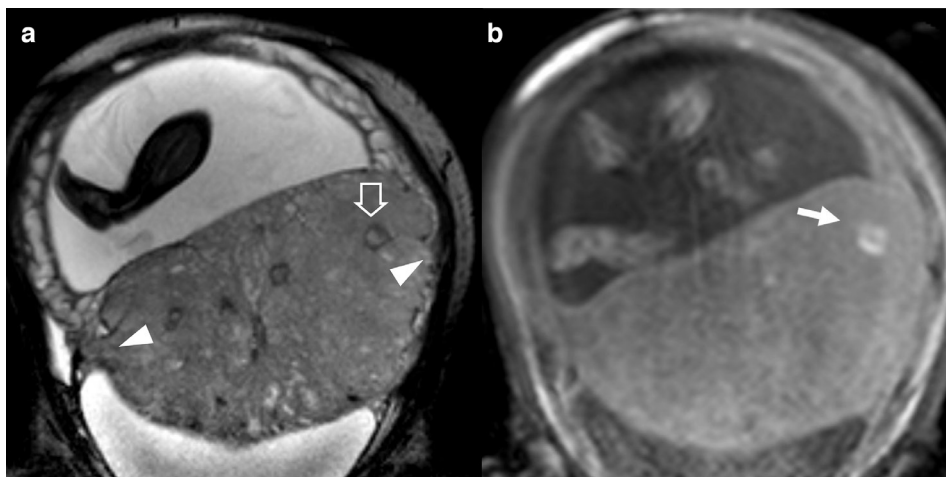
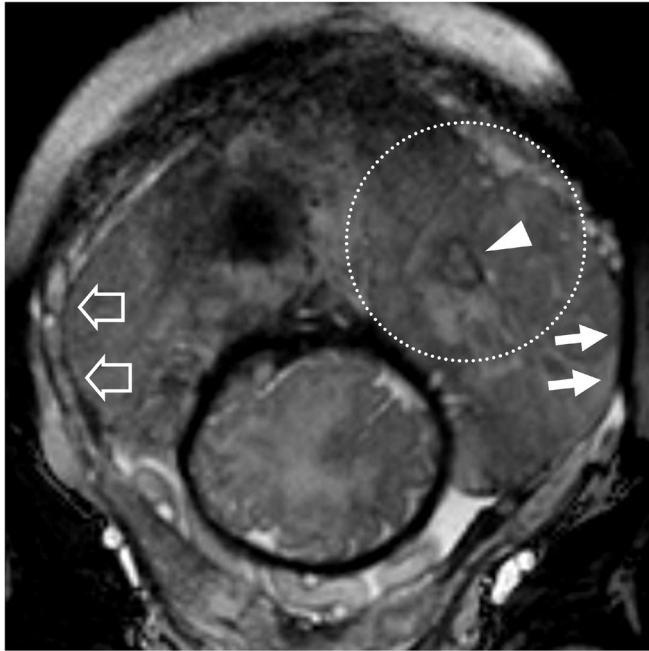


Figure 5. patient n° 5, 26 y/o at 29th week, at first pregnancy, with no previous CS. Placenta previa percreta histologically confirmed.  $T_2$  weighted coronal image. Nodular black band (arrowhead) inside a highly heterogeneous portion of the placenta (white dotted circle). On the left side-of the uterus, the myometrium is interrupted (white arrows) and it is clear if compared with the opposite side-where the myometrium is normal (empty arrow). CS, caesarean sections.



ml,  $p = 0.0106$ ) and required 794.55 ml red cells transfusion more (CI 0.95: 173.89–1415.21 ml,  $p = 0.0082$ ). They spent two more days in intense care unit (CI 0.95: 0.17–3.89,  $p = 0.0174$ ), stayed 29.67 more days in hospital (CI 0.95: 2.33–57.00) and had a relative risk of being transfused of 2.75 ( $p = 0.051$ ). Two outcomes were worse in IR-A group in comparison to IR-NA group: haemoglobin lost in operating room with a difference of 0.22 g (CI 0.95: -1.47 -1.91 g,  $p = 0.3894$ ) and the relative risk of being hysterectomised which was 0.81 because 81.18%

of IR-A females needed an hysterectomy in comparison to only 66.67% of IR-NA females.

In assisted patients mean time of radiation exposure was 9.84 min and mean administrated dose was 121.90 mGy\*cm.

## DISCUSSION

MRI allows to describe the exact position of the placenta and its eventual adhesion disorders or extension through the myometrium with high reliability. MRI proved, also in the present study, to be a useful tool in the diagnosis of IP and it should be performed in presence of risk factors, doubtful placental localisation and suspected IP as already stated in international guidelines.<sup>22</sup> In the reported case series, MRI was extremely accurate and reproducible in the diagnosis of IP with 100% sensitivity and 92.31% specificity. MRI had an NPV of 100% and a PPV of 92.9%. A high PPV is particularly important in order not to lose any eventual affected patients, while a high PPV allows to avoid over diagnosis and inappropriate IR procedures. Diagnostic accuracy in the recognition of PP is lower, but this result may be affected by the low prevalence in our series. Moreover, MRI diagnosis of IP has a very good reproducibility among dedicated radiologists.

In the present study, the reliability of eight specific MRI features have been evaluated in the diagnosis of IP. The diagnostic performance described in Table 3 refers to an MRI exam performed on females with high clinical and sonographic risk of IP.

Two signs can be considered reliable also when present alone: placental heterogeneity and interruption of myometrial layer. Placental heterogeneity regards pathological development of placenta during pregnancy and it is typical of IP. Interruption of myometrial layer indirectly refers to the disruption of muscular fibres, which are substituted by placental elements (Figure 1) and it is a precise sign of PI or PP depending to the extension of placenta up to or beyond the uterine serosa (Figure 6). Another sign suggestive of PP is bladder tenting, although its reliability in our case series resulted to be quite low.

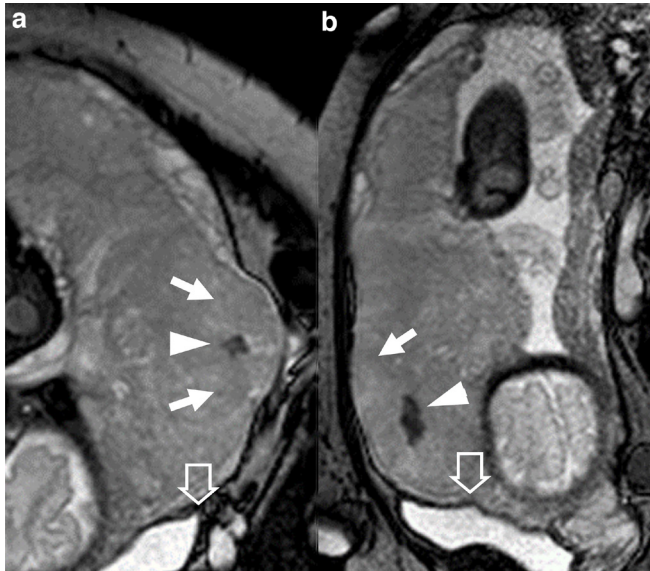
Table 4. Efficacy of interventional radiology assistance of the delivery

|                               | IR-A (11) mean    | IR-NA (3) mean    | Difference | 95% CI of the difference |         | <i>p</i> |
|-------------------------------|-------------------|-------------------|------------|--------------------------|---------|----------|
| Blood loss (ml)               | 1763.64 (±805.32) | 3033.33 (±57.74)  | 1269.70    | 225.87                   | 2313.53 | 0.0106   |
| Hb lost in operating room (g) | -1.59 (±0.96)     | -1.37 (±1.99)     | 0.22       | -1.47                    | 1.91    | 0.3894   |
| Red cells transfusion (ml)    | 305.45 (±472.79)  | 1100.00 (±173.20) | 794.55     | 173.89                   | 1415.20 | 0.0082   |
| Days in ICU (n)               | 1.00 (±0.77)      | 3.00 (±2.65)      | 2.00       | 0.17                     | 3.83    | 0.0174   |
| Hospitalisation (days)        | 12.00 (±9.22)     | 41.67 (±42.44)    | 29.67      | 2.33                     | 57.00   | 0.0179   |
| Risk of transfusion (rr)      | 0.3636            | 1.0000            | 2.78       |                          |         | 0.051    |
| Risk of hysterectomy (rr)     | 0.8182            | 0.6667            | 0.81       |                          |         | 0.571    |

Hb, Haemoglobin; ICU, Intense care unit; IR-A, patients assisted with interventional radiology; IR-NA, patients not assisted with interventional radiology; rr, relative risk.

Comparison of outcomes between patients who received interventional radiology assistance and patients who did not.

Figure 6. patient 10, 26 y/o at 39th week, at third pregnancy, with two previous CS. Marginal placenta previa percreta histologically confirmed. BTFE images A) coronal, (B) sagittal. Big placental bulge (arrows), nodular T2 dark band (arrowheads), tenting of the bladder (empty arrows). BTFE, balanced turbo field-echo.



The presence of other MRI features of IP should be accurately weighted because they can either represent a sign of IP, a variance from the normality or a sign of other placental disease. In particular uterine bulging and the loss of normal uterine pear shape should be differentiated by placental bulging which can be caused by hypertrophy of a placental lobe and it is quite common at advanced gestational age. Hyperintense placental lacunae in  $T_1$  weighted sequences and dark placental bands in  $T_2$  weighted images are an expression of the same pathological process and are a sign of placental infarction, typical of IP. They can be seen simultaneously or not depending on the timing of the haemorrhage. Hyperintense placental lacunae should be differentiated by haemorrhagic outcome of a placental abruption, because the former is intraplacental and the latter entities usually lies between placenta and myometrium. Dark intraplacental bands should be differentiated by placental septae, which are thinner and run through the placenta between placental lobes.

Interruption of inner myometrial layer can be considered a reliable sign of IP and in particular of PA because its pathological correlation is a disruption of decidua basalis. It has a quite low specificity because the evaluation of this thin line at advanced gestational age is not easy. Implant on uterine scar can be considered as a specific manifestation of this sign because on previous scar, the myometrium is mixed with fibrous tissue and the decidua basalis is frequently interrupted.

The main concern performing MRI and IR on pregnant females was the safety of the mother and the child. Foetal SAR was kept as low as possible to obtain a diagnostic imaging

and during IR only fluoroscopy was performed avoiding angiographic imaging. Both procedures are considered safe in the last trimester and are routinely performed in many centres. As regard to foetal SAR, it was not possible to find any clear experimental data on SAR limit or recommended values in pelvic MRI of pregnant females.<sup>31,32</sup> As regards to IR, we obtained the mean dose administered which was 121 mGy\*cm; considering the absorbed foetal dose 0.15 times the entrance skin dose,<sup>33</sup> our values can be considered safe for the mother<sup>34</sup> and the child<sup>35</sup> and in line with the available literature.<sup>36</sup>

Our results are consistent with recent studies<sup>37</sup> and metanalysis,<sup>38</sup> confirming that MRI evaluation in case of suspected IP at sonography is highly suggested. On the other hand, some authors<sup>39</sup> suggested that ultrasound is the only diagnostic tool needed in case of suspected IP when no technical difficulties, like posterior placenta and obesity are present.<sup>40</sup> We partially agree with that but, as shown in many researches through the years, MRI has also a role in defining the grade of IP<sup>41</sup> and eventual extension to other pelvic organs. Moreover, the use of MRI may reduce overdiagnosis and related costs and exposure, for example our case series, 12/26 females with high risk at targeted sonography were then correctly diagnosed as non-IP at MRI examination.

A reliable diagnosis enables to plan and perform a safe delivery in the appropriate setting, which means CS performed before the 40th week of gestational age in a third level hospital with availability of IR assistance, a maternal and neonatal intense care unit and availability of blood products. In our small group of patients diagnosed with IP at MRI, IR-assisted delivery reduced bleeding and related morbidity and length of intense care unit stay and overall hospitalisation and the administration of blood products. Two outcomes were worse in the IR-A group: haemoglobin loss in operative room and relative risk of being hysterectomised, although without statistical significance. The count of haemoglobin loss in operating room is probably biased by the fact that patients with higher blood loss, typically IR non-assisted females group, received red cells transfusion, which lowered the global reduction of haemoglobin count. On the other hand, in patients with less blood loss, typically IR assisted females, surgeons and anaesthesiologist tried to avoid risks deriving from transfusion by delaying and frequently avoiding that. The higher relative risk of hysterectomy in the IR-assisted group is related to the aim of reducing patient morbidity and not necessarily to preserve uterus, especially in females with high maternal age and/or with a high number of previous caesarean deliveries and surgical uterine procedures.

A limitation of our study is the low number of patients included and especially the low number of females affected whom IR assistance was possible. Females who did not received an IR assistance due emergency delivery had an overall worse condition related also to the emergency delivery and that could have biased our results. No maternal or foetal complication were reported.

**ACKNOWLEDGMENT**

ShanikoKaleci, PhD (University of Modena and Reggio Emilia,

Departement of Dermatology) assisted Filippo Monelli MD in the execution and validation of statistical analysis.

**REFERENCES**

1. Jauniaux E, Collins S, Burton GJ. Placenta accreta spectrum: pathophysiology and evidence-based anatomy for prenatal ultrasound imaging. *Am J Obstet Gynecol* 2018; **218**: 75–87. doi: <https://doi.org/10.1016/j.ajog.2017.05.067>
2. Jauniaux E, Jurkovic D. Placenta accreta: pathogenesis of a 20th century iatrogenic uterine disease. *Placenta* 2012; **33**: 244–51. doi: <https://doi.org/10.1016/j.placenta.2011.11.010>
3. Kaplan CG. *Color Atlas of Gross Placental Pathology*. 2nd edn: Springer; 2007.
4. Faye-Petersen OM, Heller DS, Joshi VV. *Handbook of Placental Pathology*. 2nd edn: Taylor & Francis; 2006.
5. Creanga AA, Syverson C, Seed K, Callaghan WM. Pregnancy-Related mortality in the United States, 2011–2013. *Obstet Gynecol* 2017; **130**: 366–73. doi: <https://doi.org/10.1097/AOG.0000000000002114>
6. Mehrabadi A, Hutcheon JA, Liu S, Bartholomew S, Kramer MS, Liston RM, et al. Contribution of placenta accreta to the incidence of postpartum hemorrhage and severe postpartum hemorrhage. *Obstet Gynecol* 2015; **125**: 814–21. doi: <https://doi.org/10.1097/AOG.0000000000000722>
7. Stivanello E, Knight M, Dallolio L, Frammartino B, Rizzo N, Fantini MP. Peripartum hysterectomy and cesarean delivery: a population-based study. *Acta Obstet Gynecol Scand* 2010; **89**: 321–7. doi: <https://doi.org/10.3109/00016340903508627>
8. Wu S, Kocherginsky M, Hibbard JU. Abnormal placentation: twenty-year analysis. *Am J Obstet Gynecol* 2005; **192**: 1458–61. doi: <https://doi.org/10.1016/j.ajog.2004.12.074>
9. Morlando M, Sarno L, Napolitano R, Capone A, Tessitore G, Maruotti GM, et al. Placenta accreta: incidence and risk factors in an area with a particularly high rate of cesarean section. *Acta Obstet Gynecol Scand* 2013; **92**: 457–60. doi: <https://doi.org/10.1111/aogs.12080>
10. Thurn L, Lindqvist PG, Jakobsson M, Colmorn LB, Klungsoyr K, Bjarnadóttir RI, et al. Abnormally invasive placenta-prevalence, risk factors and antenatal suspicion: results from a large population-based pregnancy cohort study in the Nordic countries. *BJOG* 2016; **123**: 1348–55. doi: <https://doi.org/10.1111/1471-0528.13547>
11. Silver RM, Landon MB, Rouse DJ, Leveno KJ, Spong CY, Thom EA, et al. Maternal morbidity associated with multiple repeat cesarean deliveries. *Obstet Gynecol* 2006; **107**: 1226–32. doi: <https://doi.org/10.1097/01.AOG.0000219750.79480.84>
12. Li K, Zou Y, Sun J, Wen H. Prophylactic balloon occlusion of internal iliac arteries, common iliac arteries and infrarenal abdominal aorta in pregnancies complicated by placenta accreta: a retrospective cohort study. *Eur Radiol* 2018; **28**: 4959–67. doi: <https://doi.org/10.1007/s00330-018-5527-7>
13. Angileri SA, Mailli L, Raspanti C, Ierardi AM, Carrafiello G, Belli A-M. Prophylactic occlusion balloon placement in internal iliac arteries for the prevention of postpartum haemorrhage due to morbidly adherent placenta: short term outcomes. *Radiol Med* 2017; **122**: 798–806. doi: <https://doi.org/10.1007/s11547-017-0777-z>
14. Giurazza F, Albano G, Valentino L, Schena E, Capussela T, Di Pasquale MA, et al. Predelivery uterine arteries embolization in patients affected by placental implant anomalies. *Radiol Med* 2018; **123**: 71–8. doi: <https://doi.org/10.1007/s11547-017-0796-9>
15. Clausen C, Stensballe J, Albrechtsen CK, Hansen MA, Lönn L, Langhoff-Roos J. Balloon occlusion of the internal iliac arteries in the multidisciplinary management of placenta percreta. *Acta Obstet Gynecol Scand* 2013; **92**: 386–91. doi: <https://doi.org/10.1111/j.1600-0412.2012.01451.x>
16. Soro M-AP, Denys A, de Rham M, Baud D. Short & long term adverse outcomes after arterial embolisation for the treatment of postpartum haemorrhage: a systematic review. *Eur Radiol* 2017; **27**: 749–62. doi: <https://doi.org/10.1007/s00330-016-4395-2>
17. Manninen A-L, Ojala K, Nieminen MT, Perälä J. Fetal radiation dose in prophylactic uterine arterial embolization. *Cardiovasc Intervent Radiol* 2014; **37**: 942–8. doi: <https://doi.org/10.1007/s00270-013-0751-7>
18. D'Antonio F, Palacios-Jaraquemada J, Lim PS, Forlani F, Lanzone A, Timor-Tritsch I, et al. Counseling in fetal medicine: evidence-based answers to clinical questions on morbidly adherent placenta. *Ultrasound Obstet Gynecol* 2016; **47**: 290–301. doi: <https://doi.org/10.1002/uog.14950>
19. D'Antonio F, Iacovella C, Bhide A. Prenatal identification of invasive placentation using ultrasound: systematic review and meta-analysis. *Ultrasound Obstet Gynecol* 2013; **42**: 509–17. doi: <https://doi.org/10.1002/uog.13194>
20. Bowman ZS, Eller AG, Kennedy AM, Richards DS, Winter TC, Woodward PJ, et al. Accuracy of ultrasound for the prediction of placenta accreta. *Am J Obstet Gynecol* 2014; **211**: 177.e1–177.e7. doi: <https://doi.org/10.1016/j.ajog.2014.03.029>
21. D'Antonio F, Iacovella C, Palacios-Jaraquemada J, Bruno CH, Manzoli L, Bhide A. Prenatal identification of invasive placentation using magnetic resonance imaging: systematic review and meta-analysis. *Ultrasound Obstet Gynecol* 2014; **44**: 8–16. doi: <https://doi.org/10.1002/uog.13327>
22. Cantwell R, Clutton-Brock T, Cooper G, Dawson A, Drife J, Garrod D, et al. Saving mothers' lives: reviewing maternal deaths to make motherhood safer: 2006–2008. The eighth report of the Confidential enquiries into maternal deaths in the United Kingdom. *BJOG* 2011; **118 Suppl 1**(Suppl 1): 1–203. doi: <https://doi.org/10.1111/j.1471-0528.2010.02847.x>
23. Horowitz JM, Berggruen S, McCarthy RJ, Chen MJ, Hammond C, Trinh A, et al. When timing is everything: are placental MRI examinations performed before 24 weeks' gestational age reliable? *AJR Am J Roentgenol* 2015; **205**: 685–92. doi: <https://doi.org/10.2214/AJR.14.14134>
24. Baughman WC, Corteville JE, Shah RR. Placenta accreta: spectrum of US and MR imaging findings. *Radiographics* 2008; **28**: 1905–16. doi: <https://doi.org/10.1148/rg.287085060>
25. Lax A, Prince MR, Mennitt KW, Schwebach JR, Budorick NE. The value of specific MRI features in the evaluation of suspected placental invasion. *Magn Reson Imaging* 2007; **25**: 87–93. doi: <https://doi.org/10.1016/j.mri.2006.10.007>
26. Alamo L, Anaya A, Rey J, Denys A, Bongartz G, Terraz S, et al. Detection of suspected placental invasion by MRI: do the results depend on observer' experience? *Eur J Radiol* 2013; **82**: e51–7. doi: <https://doi.org/10.1016/j.ejrad.2012.08.022>



27. Bour L, Placé V, Bendavid S, Fargeaudou Y, Portal J-J, Ricbourg A, et al. Suspected invasive placenta: evaluation with magnetic resonance imaging. *Eur Radiol* 2014; **24**: 3150–60. doi: <https://doi.org/10.1007/s00330-014-3354-z>
28. Yang A, Xiao XH, Wang ZL, Wang ZY, Wang KY. T2-Weighted balanced steady-state free precession MRI evaluated for diagnosing placental adhesion disorder in late pregnancy. *Eur Radiol* 2018; **28**: 3770–8. doi: <https://doi.org/10.1007/s00330-018-5388-0>
29. Dannheim K, Shainker SA, Hecht JL. Hysterectomy for placenta accreta; methods for gross and microscopic pathology examination. *Arch Gynecol Obstet* 2016; **293**: 951–8. doi: <https://doi.org/10.1007/s00404-015-4006-5>
30. Benirschke K, Burton GJ, Baergen RN. *Pathology of the Human Placenta*. 6th edn: Springer; 2012.
31. American College of Radiology, ACR ACR–SPR practice parameter for the safe and optimal performance of fetal magnetic resonance imaging (MRI). *American College of Radiology* 2015; **1076**: 1–14.
32. Ray JG, Vermeulen MJ, Bharatha A, Montanera WJ, Park AL. Association between MRI exposure during pregnancy and fetal and childhood outcomes. *JAMA* 2016; ; **316**: 952–616. doi: <https://doi.org/10.1001/jama.2016.12126>
33. El-Khoury GY, Madsen MT, Blake ME, Yankowitz J. A new pregnancy policy for a new era. *AJR Am J Roentgenol* 2003; **181**: 335–40. doi: <https://doi.org/10.2214/ajr.181.2.1810335>
34. Nikolic B, Spies JB, Lundsten MJ, Abbara S. Patient radiation dose associated with uterine artery embolization. *Radiology* 2000; **214**: 121–5. doi: <https://doi.org/10.1148/radiology.214.1.r00ja24121>
35. ICRP Publication The 2007 recommendations of the International Commission on radiological protection. *Annals of ICRP* **103**.
36. Chen L, Wang X, Wang H, Li Q, Shan N, Qi H, et al. Clinical evaluation of prophylactic abdominal aortic balloon occlusion in patients with placenta accreta: a systematic review and meta-analysis. *BMC Pregnancy Childbirth* 2019; ; **19**: 3015. doi: <https://doi.org/10.1186/s12884-019-2175-0>
37. Maurea S, Romeo V, Mainenti PP, Ginocchio MI, Frauenfelder G, Verde F, et al. Diagnostic accuracy of magnetic resonance imaging in assessing placental adhesion disorder in patients with placenta previa: correlation with histological findings. *Eur J Radiol* 2018; **106**: 77–84. doi: <https://doi.org/10.1016/j.ejrad.2018.07.014>
38. Familiari A, Liberati M, Lim P, Pagani G, Cali G, Buca D, et al. Diagnostic accuracy of magnetic resonance imaging in detecting the severity of abnormal invasive placenta: a systematic review and meta-analysis. *Acta Obstet Gynecol Scand* 2018; **97**: 507–20. doi: <https://doi.org/10.1111/aogs.13258>
39. Berkley EM, Abuhamad AZ. Prenatal diagnosis of placenta accreta: is sonography all we need? *J Ultrasound Med* 2013; **32**: 1345–50. doi: <https://doi.org/10.7863/ultra.32.8.1345>
40. McLean LA, Heilbrun ME, Eller AG, Kennedy AM, Woodward PJ. Assessing the role of magnetic resonance imaging in the management of gravid patients at risk for placenta accreta. *Acad Radiol* 2011; **18**: 1175–80. doi: <https://doi.org/10.1016/j.acra.2011.04.018>
41. Aitken K, Allen L, Pantazi S, Kingdom J, Keating S, Pollard L, et al. Mri significantly improves disease staging to direct surgical planning for abnormal invasive placentation: a single centre experience. *J Obstet Gynaecol Can* 2016; **38**: 246–51. doi: <https://doi.org/10.1016/j.jogc.2016.01.005>